J. Mol. Biol. (1974) **85**, 501–532

Non-random Circular Permutation of Phage P22 DNA

BIK-KWOON TYE, JOEL A. HUBERMAN AND DAVID BOTSTEIN

Department of Biology
Massachusetts Institute of Technology
Cambridge, Mass. 02139, U.S.A.

(*Received 24 September 1973*)

Phage P22 is known to have a linear duplex chromosome that is circularly permuted and terminally repeated. We have found, by constructing a partial denaturation map of mature P22 DNA, that circular permutation in P22 DNA is restricted: all of the ends of the mature DNA fall within 20% of each other on the physical map. The limited distribution of ends can be explained by the "headful" packaging model of Streisinger *et al.* (1967), with the additional specifications that:

(a) the intracellular precursor DNA is no longer than ten times the length of mature phage DNA;

(b) encapsulation of DNA starts at a unique site;

(c) encapsulation proceeds sequentially therefrom.

This model is supported by the denaturation maps of two deletion phage DNAs. We found, as expected from our model, that the extent of permutation is a direct function of the length of terminal repetition. An independent demonstration of this relation between permutation and terminal repetition was done by denaturation–self-reannealing experiments using wild type and deletion phage DNAs.

In the case of phage with large terminal repetitions (16%), we can discern discrete classes of molecules (using denaturation mapping), which we interpret as the first, second, etc. headful cut from the intracellular DNA concatemer.

1. Introduction

Most of the well-known bacteriophages that have linear duplex chromosomes can be divided into three broad classes on the basis of chromosome type. One class has chromosomes with unique ends and short, single-stranded cohesive extensions; this class includes coliphages λ (Hershey *et al.*, 1963; Wu & Kaiser, 1968; Wu & Taylor, 1971), P2 (Mandel, 1967), 186 (Baldwin *et al.*, 1966), and φ80 (Yamagashi *et al.*, 1965). A second class has unique ends but duplex terminal repetitions of substantial length; this class is exemplified by the T-odd coliphages T1 (MacHattie *et al.*, 1972), T3, T7 (Ritchie *et al.*, 1967) and T5 (Rhoades & Rhoades, 1972). Finally, there is a class that has circularly permuted ends and substantial duplex terminal repetition. This class includes the *Salmonella* temperate phage P22 (Rhoades *et al.*, 1968), coliphage P1 (Ikeda & Tomizawa, 1968), coliphage 15 (Lee *et al.*, 1970) and the T-even coliphages (MacHattie *et al.*, 1967). The form of the DNA inside the phage head does not seem to reflect primarily the form of the intracellular replicating DNA from which it is derived, since it has been shown that various phages seem to have

roughly similar concatemeric intracellular replicative forms: T4 (Frankel, 1966a,*b*,*c*), λ (Smith & Skalka, 1966; Salzman & Weissbach, 1967; Skalka *et al.*, 1972), T7 (Thomas *et al.*, 1968) and P22 (Botstein & Levine, 1968*a*,*b*). Instead, it seems that the final product inside the phage head might reflect the mechanism by which the mature DNA is processed or cut from the overlength concatemeric DNA precursor. In all phages studied, this cutting event is directly related to the encapsulation of the DNA. It is known that phage λ head mutants accumulate high molecular weight concatemeric DNA and fail to form new phage particles on infection (Wake *et al.*, 1972; Skalka *et al.*, 1972). Botstein *et al.* (1973) have recently published evidence for an intimate relation between head assembly and DNA encapsulation in phage P22. A similarly close relation between head assembly and DNA encapsulation has also been found in the more complex coliphage T4 (Laemmli, 1970; Luftig *et al.*, 1971; Showe & Black, 1973). In all of these cases, there is evidence for direct involvement of a precursor of the morphogenetic phage head in the encapsulation of concatemeric DNA; such a P22 head precursor has recently been identified and characterized in P22 (King *et al.*, 1973; Botstein *et al.*, 1973).

Phage P22 is a temperate phage of *Salmonella typhimurium*. Its chromosome is a linear duplex DNA molecule that measures approximately 15 μm (see preceding paper, Tye *et al.*, 1974) and has a molecular weight of 27×10^6 (Rhoades *et al.*, 1968). Like the T-even coliphages, it has a circular genetic map (Gough & Levine, 1968). Its chromosome is circularly permuted with a terminal repetition of approximately 2% (Rhoades *et al.*, 1968; Tye *et al.*, 1974).

Streisinger *et al.* (1967) proposed a model that accounts for the generation of these circularly permuted and terminally repeated DNA molecules. They envisioned that the intracellular precursor DNA molecules are repeating polymers (concatemers) of the phage genome. Streisinger suggested that the length of the DNA packaged inside a phage head is determined by the amount of DNA that can fit into the head; i.e. DNA is packaged by the headful. If the genome length is smaller than the headful, a terminally repeated molecule will be produced when a headful is cut from the concatemer. A headful in the case of P22 is equivalent to the complete wild-type phages genome plus 2%. Streisinger *et al.* (1967) showed by genetic means that phages with deletions in their genome have a longer terminal repetition. Using more direct physical methods, we have confirmed this result in the case of P22 (Tye *et al.*, 1974), showing quantitatively that the genome size determines directly the size of the terminal repetition.

The generation of circular permutation in the DNA of the progeny of a single phage particle is nicely explained by the Streisinger model as well. If headfuls are cut from the concatemer at different genetic points, circular permutation (as well as terminal repetition) results. However, the Streisinger model does not specify whether the headful encapsulation mechanism cuts out headfuls randomly from the concatameric precursor or whether headfuls are cut sequentially once packaging begins on a concatemer. If the concatameric DNA were very long or if the sequential cutting could initiate from any random point, one would expect the resulting population of DNA molecules to have randomly permuted ends. If, however, the cutting were always initiated at a specific site and the precursor DNA were of limited length, then one could distinguish the random cutting mechanism from the sequential cutting mechanism, because each sequential headful would have ends differing from the preceding headful by the length of the terminal repetition. Thus, if the concatemer

were ten headfuls long and the terminal repetition were 2%, then the total distance between the ends of the first and last headful would only span 20% of the genome. A comparison between random and unique site-sequential encapsulation is shown in Figure 1.

In an effort to construct a partial denaturation map of phage P22 chromosomes, we observed that the extent of permutation in a population of phage P22 chromosomes is very restricted. This immediately called into question the notion of a totally random packaging mechanism. In this paper we present evidence leading to the conclusion that DNA encapsulation is initiated at a specific site on the intracellular precursor DNA and proceeds unidirectionally and sequentially. All the evidence presented in this paper is provided by two techniques, namely partial denaturation mapping and denaturation–self-reannealing of DNA molecules.

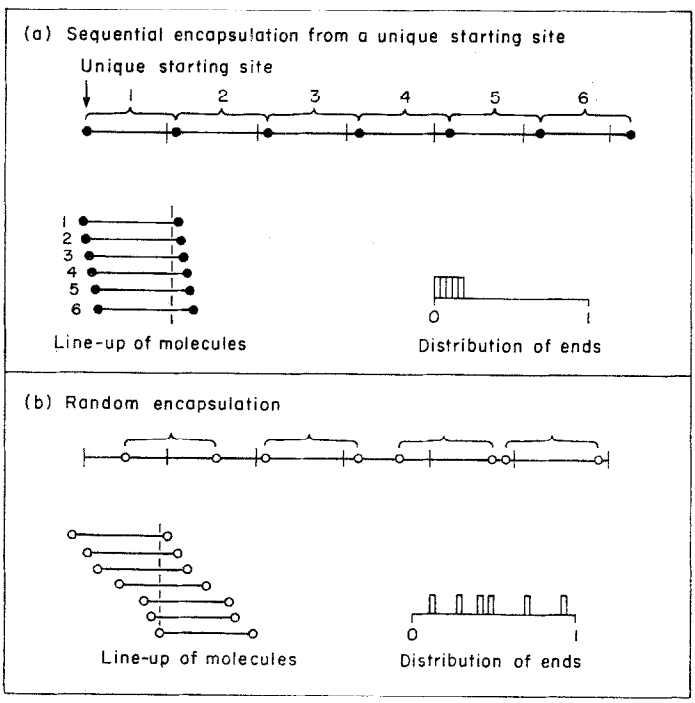

FIG. 1. (a) Diagram showing that if the intracellular, multiple-length precursor is only long enough for a small number of headfuls to be made, sequential encapsulation from a unique starting site results in a restricted distribution of ends.

(b) Random encapsulation results in a random distribution of ends.

2. Materials and Methods

All bacterial strains, phage strains, media, and phage DNA preparations are as described in the preceding paper (Tye *et al.*, 1974).

(a) *Partial denaturation of phage DNA*

(i) *Formamide denaturation of DNA*

The method used has been described by Wolfson *et al.* (1972). The DNA molecules are partially denatured by spreading the sample in the presence of a high concentration of formamide. The spreading solution consists of 85 μl of 99% formamide (Matheson, Coleman and Bell), 10 μl of 1 M-Tris·HCl (pH 8·5), 5 μl of glass-distilled water, 1 μl of DNA

(A_{260} = 0·355) in 0·01 M-Tris·HCl, 1 mM-EDTA and 1 μl of a solution of 2 mg horse heart cytochrome *c*/ml (Sigma Chemical Company). The spreading solution is incubated for about 30 min at room temperature before the addition of the cytochrome *c*. The final concentration of formamide in the solution is 83%. The solution is spread on a hypophase of 50% formamide in 0·01 M-Tris·HCl (pH 8·5). Spreading is done at room temperature.

(ii) *Alkali denaturation of DNA molecules*

The method used is a modification of that described by Inman & Schnös (1970). A buffer solution (0·02 M-Na_2CO_3, 0·005 M-EDTA, 11% formaldehyde) was adjusted to the desired pH by addition of 5 M-NaOH. The spreading solution consists of 10 μl of DNA at A_{260} = 0·1, 25 μl of 0·02 M-NaCl, 0·005 M-EDTA (pH 7·4) and 15 μl of the high-pH buffer (usually near pH 11·3). The solution is incubated for 30 min at 23°C, cooled in ice for 5 min, after which 50 μl of redistilled formamide and 2 μl of cytochrome *c* (2 mg/ml) are added and the spreading solution is left at room temperature for a further 5 to 10 min before spreading on a hypophase of distilled water. Electron microscope grids are coated with a Parlodion film without carbon; spreading is done on a slide and trough (Kleinschmidt, 1968).

(b) *Denaturation–reannealing experiment*

As described in the preceding paper (Tye *et al.*, 1974).

(c) *Data analysis*

(i) *Measurements*

To map the regions of P22 DNA that preferentially melt out in the partially denatured molecules, the molecules were photographed and printed at a final magnification of 37,500× and traced on a Computek analog–digital conversion device attached to a PDP9 computer. All lengths were normalized to the total length of the P22 chromosome.

(ii) *Alignment of partial denaturation maps*

Sets of P22 DNA molecules (unlike λ, P2, T7 or ϕ186 DNA molecules) are permuted. In order to compute a partial denaturation histogram for P22, molecules have to be lined up with respect to their partial denaturation pattern rather than from their ends. This was done by plotting each denaturation map on a strip of graph paper and aligning the strips by eye for best fit with each other. Often it was useful to attach 2 copies of the map end to end (removing an amount corresponding to the terminal repetition) in order to align substantially permuted maps. Left to right orientation was determined by trial of each orientation for each case; fortunately, the asymmetry of the maps is such that this decision was almost always unambiguous. In the final adjustment of the alignment of the partial denaturation maps, a characteristic feature of each set of maps was used as a point of reference, as indicated on each map. The use of different references in different sets of maps may contribute to some differences in the profiles of the different histograms of partial denaturation maps; however, the fact that the maps are grossly similar even though different features were used for each alignment shows that the histograms are nearly independent of the reference point.

During the preparation of this manuscript, it became possible to align the partial denaturation maps objectively by use of a computer. The method and the fact that the computer and visual alignments were virtually identical are briefly reported in the Appendix.

Since the denaturation size and position data were normalized to the total length of each molecule, the scale for all the maps and histograms is in fractions of a P22 *mature* length. The total length is shown in the histograms as the *genome* length, which is equal to 1 — (fractional length of the terminal repetition). All the histograms are oriented to facilitate comparison of the maps (see Fig. 13).

It is important that the population of molecules considered be intact, because molecules broken near their ends would not be recognized as broken. In the preceding paper,

we found that the circumference of homoduplex circular DNA can be determined to $\pm 3\%$. However, in the case of partially denatured DNA molecules, the accuracy decreases to $\pm 7\%$. Rather than attribute this to broken molecules, we would like to attribute the larger variation in total map length to the inaccuracy in measuring denatured regions that appear to be more twisted than undenatured regions and, therefore, more difficult to trace accurately. Also, as determined by Freifelder *et al.* (1964), the single-stranded circular ϕX DNA molecule is longer than the double-stranded replicative form, and we did not correct for this difference in our measurements; therefore, molecules with larger amounts of denaturation would appear to be longer. Inman (1967) has found in determining the partial denaturation map of λ that a variation in length of at least $\pm 1{\cdot}0$ μm ($\pm 5{\cdot}7\%$) is necessary to contain 85% of the whole molecules. We consider that our finding of $\pm 7\%$ variation (amounting to $\pm 1{\cdot}1$ μm) within the total population is a legitimate variation amongst whole molecules.

(iii) *Computation*

Each set of maps is plotted in the form of a weight-average histogram as described by Inman (1967). Each denaturation map computed by the computer gives a resolution of $0{\cdot}1\%$ of the normalized length. The histogram contains 200 rectangles corresponding to a resolution of $0{\cdot}5\%$ of the normalized length. The histograms are plotted with the terminal repetition omitted. However, since the measurements were normalized to the length of mature P22 DNA, the units in this paper are fractions of P22 *mature length*, making them 2% larger than the units in the preceding paper (Tye *et al.*, 1974), which were calculated relative to the P22 genome.

3. Results

(a) *Partial denaturation map of P22 wild-type DNA (2% terminal repetition)*

Phage P22 DNA has been shown to be circularly permuted and terminally repeated (Rhoades *et al.*, 1968). From their competition–annealing experiments, Rhoades *et al.* (1968) concluded that the number of different circular permutations in the phage P22 chromosome is large. In an attempt to construct a partial denaturation map of P22 DNA, it was rather unexpected to find that the positions of ends of a population of P22 DNA molecules were restricted within a region comprising only 20% of the total map length.

(i) *Formamide denaturation*

Wild-type P22 phage DNA was partially denatured in 83% formamide. A total of 63 molecules was photographed, traced and mapped. These maps were then lined up with respect to their denaturation patterns (Fig. 2). All denaturations were located in the middle of every molecule, no denaturations were observed at either end of each molecule. A weight-average denaturation histogram of this set of maps aligned according to denaturation patterns is shown in Figure 3(b). There appear to be three major denaturation sites. The positions of molecular ends were plotted as a second histogram with respect to the denaturation map shown in Figure 3. It is clear from Figure 3 that the ends are clustered in a region covering only about 20% of the map. Since this result was quite unexpected, and because the alignment of a set of DNA molecules by their denaturation pattern might depend on the subjectivity of the experimenter, an independent set of denaturation maps of wild-type P22 DNA was made. This time, the molecules were denatured to a smaller extent by a different method of denaturation.

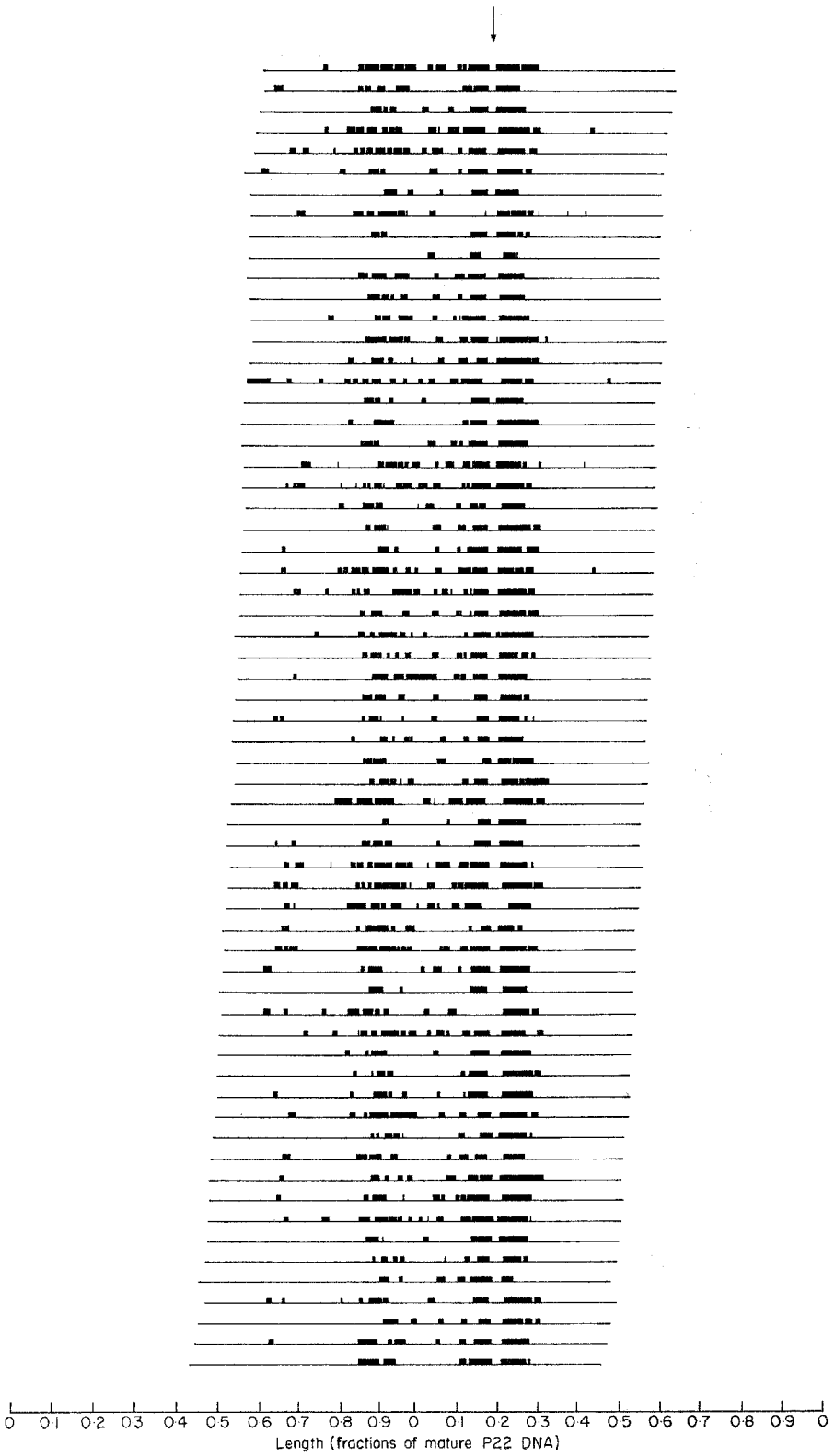
0 0·1 0·2 0·3 0·4 0·5 0·6 0·7 0·8 0·9 0 0·1 0·2 0·3 0·4 0·5 0·6 0·7 0·8 0·9 0
Length (fractions of mature P22 DNA)

FIG. 2.

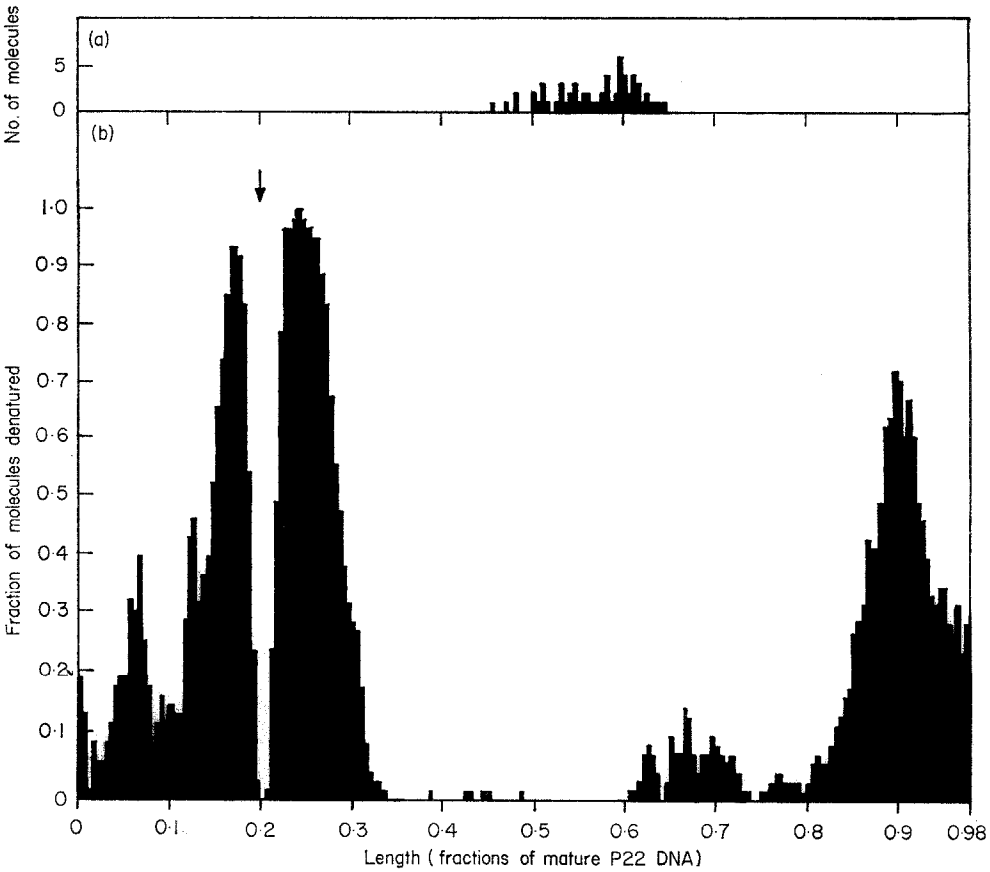

FIG. 3. (a) Histogram of the distribution of the ends of the molecules with respect to the denaturation map. The positions of ends are positions of the right ends in the alignment (see Fig. 2). The distribution of ends is non-random, clustering within 20% of the map length.

(b) Histograms of the partial denaturation maps of P22 wild-type DNA (in Fig. 2) showing the positions and frequency of the denatured sites. The x-axis is plotted as a function of the genome length such that the terminal repetition is not included in the map range, making the total length 98% P22. This is done by taking out the amount of terminal repetition (2%) from each molecule, all from the same end (left end in Fig. 2). The arrow indicates the reference for the alignment.

(ii) *Alkali denaturation*

Wild-type P22 DNA was partially denatured at pH 11·33 for 30 minutes at room temperature. A total of 35 molecules was photographed, traced and mapped. They were lined up with respect to their denaturation pattern (Fig. 4). Again, as in the formamide denaturation maps, the ends were limited to a region covering about 20% of the map. The two partial denaturation histograms produced by the formamide

FIG. 2. Partial denaturation maps of P22 wild-type DNA denatured in the presence of 83% formamide for 30 min under the conditions described in Materials and Methods. All molecules are normalized to 100% P22 mature DNA length and the length distribution of the 63 molecules measured is (100±6·7)%. The arrow indicates the reference (a characteristic gap between 2 denaturation sites) of the alignment. The maps are aligned in such a way that molecules with ends closest to one another are adjacent. The methods for left to right orientation are described in Materials and Methods, section (c)(ii).

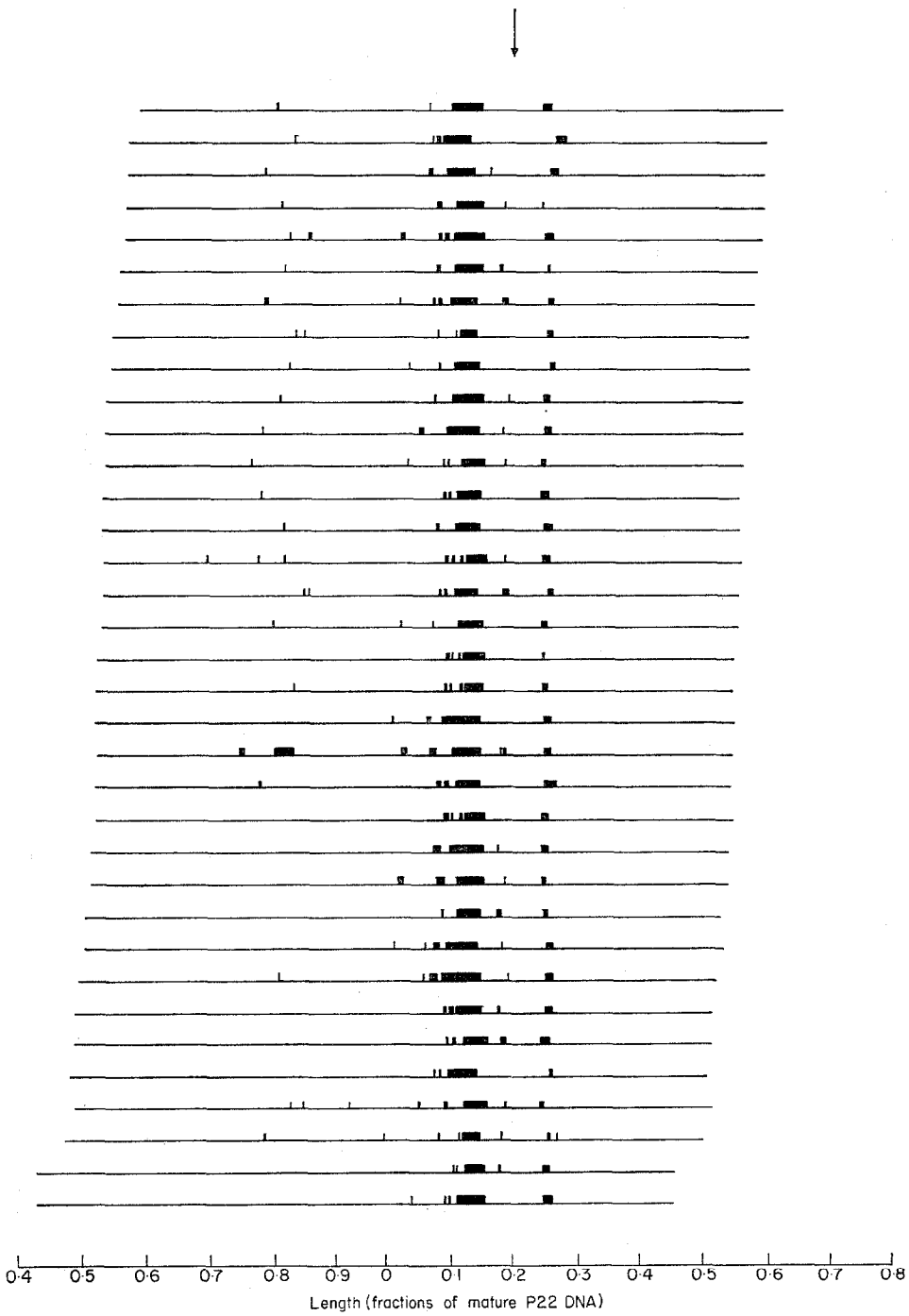

FIG. 4. Partial denaturation maps of P22 wild-type DNA denatured at pH 11·33 for 30 min at room temperature. The length distribution of the 35 molecules measured is $(100 \pm 5{\cdot}5)\%$. The arrow indicates the reference for the alignment.

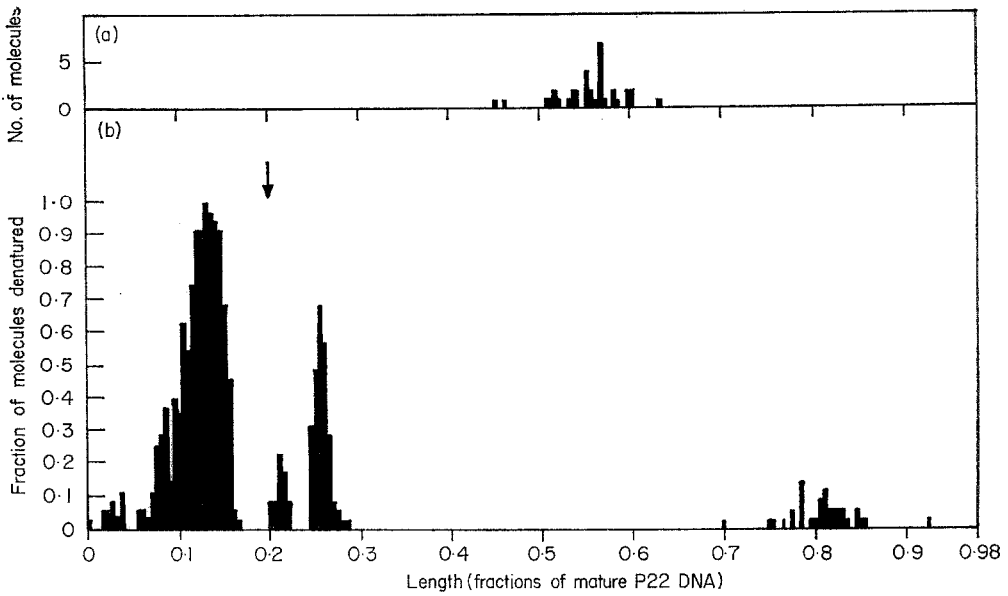

FIG. 5. (a) Histogram of the distribution of ends of the molecules with respect to the denaturation map. The position of ends is the same distance away from the 2 major denaturation sites as in Fig. 3. The ends are found to be clustered within 20% of the map length.

(b) Histograms of the partial denaturation maps of P22 wild-type DNA (in Fig. 4). The map length is plotted as 98% P22 as in Fig. 3. The arrow indicates the reference for the alignment.

and alkali denaturation methods have a very similar pattern (Fig. 5). In both cases, denaturations were located in the middle of each molecule; the ends of every molecule seem to fall within a (G + C)-rich region of the P22 genome.

The results show clearly that phage P22 DNA molecules are not randomly permuted.

(b) *The sequential encapsulation hypothesis*

One way to explain the generation of molecules with permuted but clustered ends is to hypothesize that during DNA maturation, encapsulation of DNA by phage heads takes place at a unique site and proceeds sequentially, as proposed in the Introduction (Fig. 1). If the terminal repetition is small, and the concatemer is only a few headfuls long, then sequential cutting from a unique site will result in limited circular permutation. The extent of permutation will depend on the size of the terminal repetition and the length of the concatemer.

An alternative explanation for the permuted but clustered distribution of ends is to hypothesize that the encapsulation mechanism has a specificity for certain (G + C)-rich sequences, which are clustered within a (G + C)-rich region comprising about 20% of the P22 genome.

These explanations can be distinguished by the observation that the unique site–sequential encapsulation model predicts that the extent of permutation in the

mature phage DNA should depend on the size of the terminal repetition. Alternative site-specific models should not share this property.

In the preceding paper it was shown that a deletion in the phage genome is compensated for by a lengthening of the region of terminal repetition by an amount equal to the length of the deletion and, similarly, an insertion in the phage genome is compensated for by a shortening of the region of terminal repetition. Thus, the materials for testing the unique site–sequential encapsulation hypothesis are readily available in the form of deletion and insertion mutants of P22 that have differing genome lengths and, therefore, different amounts of terminal repetition.

Figure 6 illustrates the detailed quantitative expectations of the sequential encapsulation model. One can see that the displacement of the beginning of the nth headful from the initiation site is a simple linear function of the terminal repetition characteristic of a particular phage genome. Thus, the terminal repetition in a P22

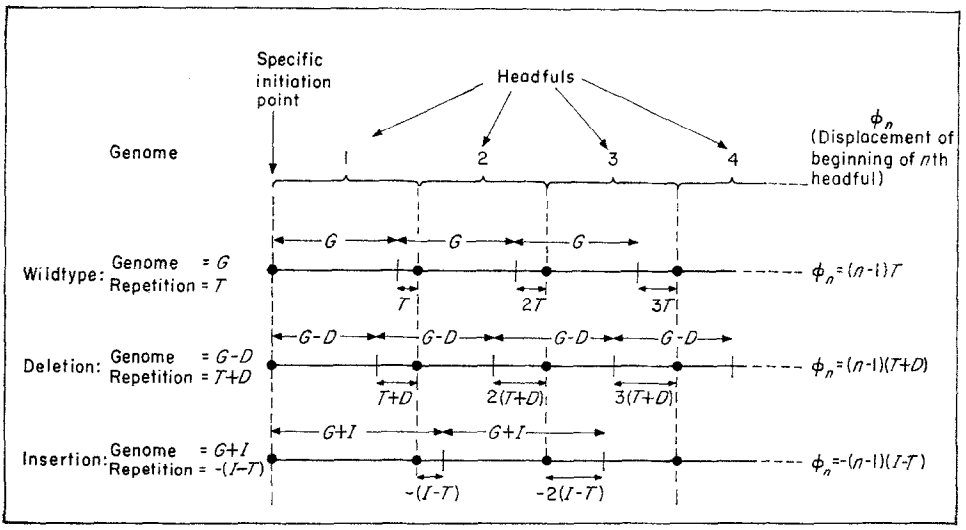

FIG. 6. Diagram illustrating the relation between genome size and the size of the terminal repetition (TR); a prediction of the model of Streisinger *et al.* (1967). Streisinger's model proposes that the length of the DNA inside a phage head is determined by the volume of the phage head. Thus, a deletion (D) in the phage genome (G) would be compensated for by a lengthening of the terminal repetition by an amount D to ($T + D$). Similarly, an insertion (I) in the phage genome would be compensated for by a shortening of the TR value by an amount I to ($T - I$). If I is greater than T, then only a fraction of the phage genome can be encapsulated by each phage head. The difference between the length of each headful ($G + T$) and the insertion phage genome ($I + G$) is $-(I - T)$; this we term negative terminal repetition.

The diagram also illustrates the relation between the size of the TR and the extent of permutation in the sequential encapsulation of DNA starting from a unique site. The longer the TR, the larger is the displacement of each sequential headful from its previous headful, resulting in a dependence of the extent of permutation on the size of the TR. For example, in the case of the wild-type phage, the 4th headful would be displaced from the first by an amount $= 3T$; i.e. the extent of permutation in 4 sequential headfuls is $3T$. In the case of the deletion phage, the extent of permutation in 4 sequential headfuls is $3(T + D)$; and in the case of the insertion phage, the extent of permutation in 4 sequential headfuls is $-3(I - T)$.

FIG. 7. Partial denaturation maps of P22*bp*1 DNA denatured at pH 11·34 for 30 min at room temperature. The length distribution of the 60 molecules measured is (100±7·5)%. The arrow indicates the reference for the alignment.

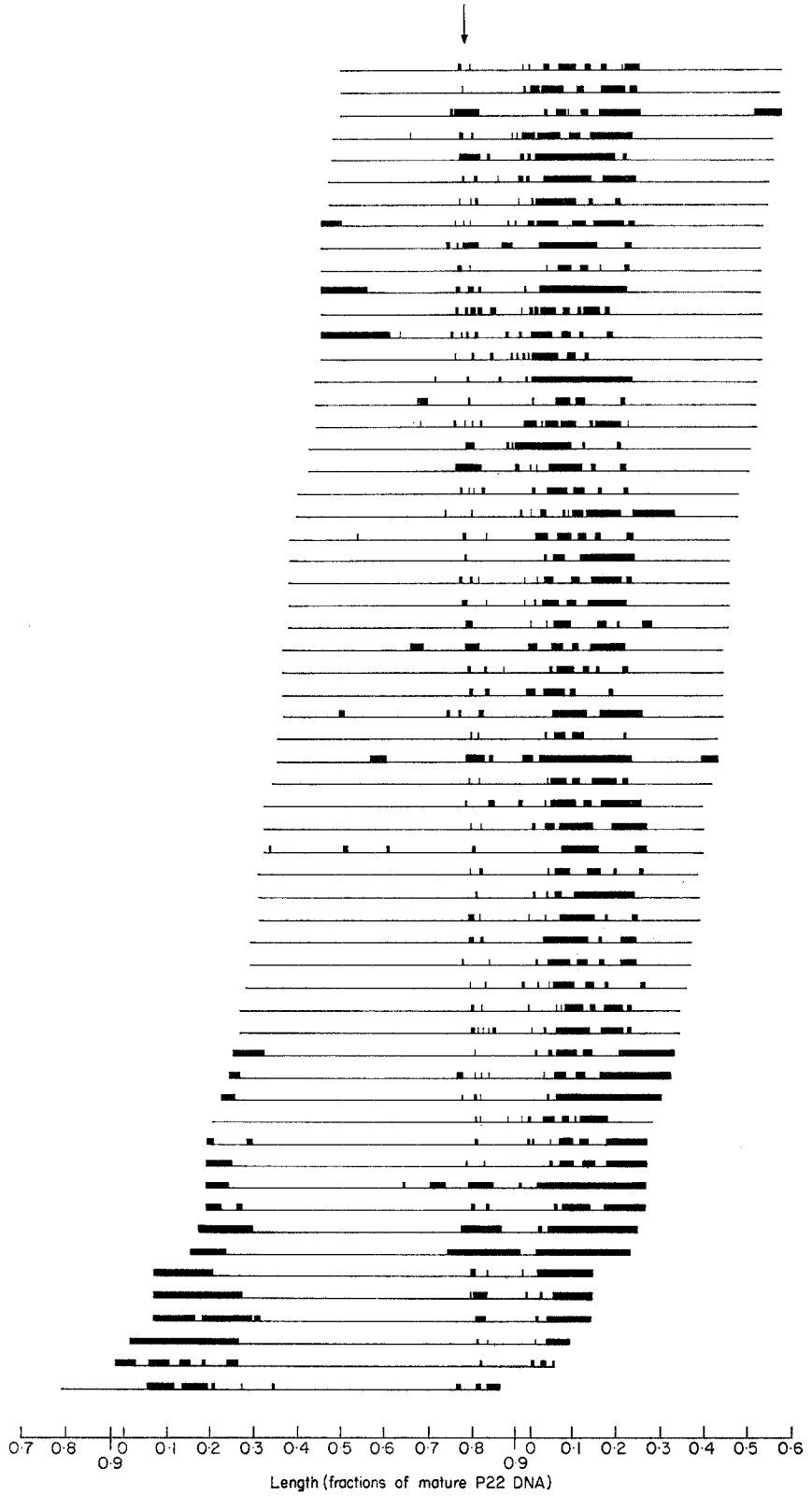
0·7 0·8 0 0·1 0·2 0·3 0·4 0·5 0·6 0·7 0·8 0 0·1 0·2 0·3 0·4 0·5 0·6
0·9
0·9
Length (fractions of mature P22 DNA)

phage with a 5% deletion is 7% (the sum of the deletion ($D = 5\%$) plus the wild-type terminal repetition ($T = 2\%$)). Then the tenth headful will begin 63% displaced from the unique site (taken as position 0% on the map). The tenth headful from a concatemer of wild-type genomes ($T = 2$) would, by a similar calculation, only be displaced 18%.

Another prediction of the model applies to phages with very large terminal repetitions. In this case, the successive headfuls will be far apart; so far, in fact, that the total errors in measurement might allow distinction of each successive class.

(c) *The partial denaturation map of P22* bp*1 DNA (7% terminal repetition)*

Phage P22*bp*1 has been described in the preceding paper (Tye *et al.*, 1974). It is a deletion–insertion phage with a net deletion of approximately 5% and consequently has a terminal repetition of approximately 7%. If the (G + C)-rich specific sequence encapsulation mechanism were correct, one would expect the histogram of the

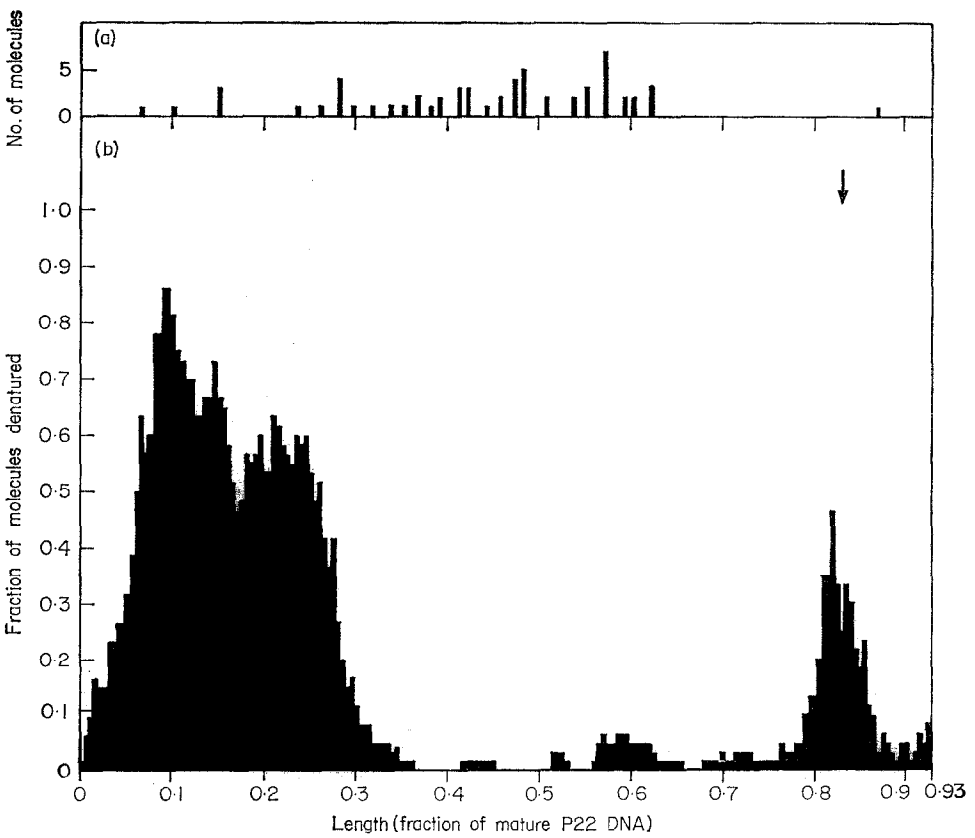

FIG. 8. (a) Histogram of the distribution of the ends of the molecules with respect to the denaturation map. The positions of ends are positions of the right ends of the molecules in Fig. 7. The distribution of ends is non-random, clustering within 60 to 70% of the map length.

(b) Histogram of the partial denaturation maps of P22*bp*1 DNA (in Fig. 7). The map length range is plotted as 93%, so that the TR value of P22*bp*1 (7%) is not included in the map length. This is done by taking out the TR of 7% from the left end of each molecule.

P22*bp*1 DNA denaturation maps to show the same clustering of ends in the (G + C)-rich region that is observed with wild-type P22 DNA. If, on the other hand, the uniquely initiated sequential encapsulation mechanism were correct, a broader distribution of ends would be expected. From the wild type partial denaturation histogram, one can estimate that approximately ten sequential headfuls are needed to yield the observed distribution of ends. Ten sequential headfuls in the case of P22*bp*1 DNA should yield a distribution of ends within 70% of the map length.

P22*bp*1 DNA was partially denatured at pH 11·34 for 30 minutes at room temperature and 60 molecules were examined. The alignment of the denaturation maps is shown in Figure 7. The histogram (Fig. 8(b)) shows that there are three major denaturation sites. The distribution of ends (Fig. 8(a)) is much less restricted than in wild type; ends are found in 60 to 70% of the map length. This eliminates the (G + C)-rich specific sequence encapsulation hypothesis, since many ends that fall within (A + T)-rich regions are found. Assuming a sequential cutting mechanism such that each cut is 7% out of phase from the previous cut, we can estimate from this the length of the intracellular precursor DNA to be not more than eight to ten times the mature DNA length. Although a distribution of classes cannot be resolved unambiguously due to the magnitude of length variation, a trend of maxima about 7% apart can barely be discerned. Even though the distribution of ends in P22*bp*1 DNA seems to be less restricted than in wild-type DNA, there is still an empty region of the map in which no ends are found (Fig. 8(b)). Ends seem to be more abundant at the right side of the end distribution and the frequency tapers off gradually at first but more rapidly towards the left side of the end distribution.

(d) *The partial denaturation map of P22*bp*5 DNA (16% terminal repetition)*

To ensure the resolution of classes of molecules that should result from sequential cutting initiated from a fixed site, partial denaturation maps were constructed from DNA of the P22*bp*5 phage described in the preceding paper. The DNA of this phage contains a large net deletion of 14%, and thus a terminal repetition of 16%. A 16% difference should be resolved even with our total experimental and manipulative error of about 8%.

P22*bp*5 DNA was partially denatured at pH 11·32 for 30 minutes at room temperature and 55 molecules were examined. Distinct classes of molecules can be resolved in both the line-up (Fig. 9) and the histogram (Fig. 10). Again, there are three major denaturation sites visible in the histogram (Fig. 10(b)). Four major classes of molecules are resolved (see section (b) in the Discussion). However, as shown in Figure 9, there may be more than four classes of molecules; overlapping classes resulting from different headfuls may be mistaken as one class. For example, class 1 and class 5 in the line-up (Fig. 9) are indistinguishable from each other. There are 20 molecules included in class 1 in the histogram, 13 molecules each are included in class 2 as well as class 3, nine molecules are included in class 4. If the most frequent class is taken as the first headful, then class 1 would correspond to the first headful; classes 2, 3 and 4 would correspond to the second, third and fourth headful, respectively. Such an assignment is strengthened by the fact that the position of class 1 coincides with the position of the clustered ends in the histogram of the wild-type P22 DNA, as well as the right side of the end distribution found with P22*bp*1 DNA. The apparent direction of encapsulation in the *bp*5 histogram would, by this assignment, be the same as that of the *bp*1 histogram.

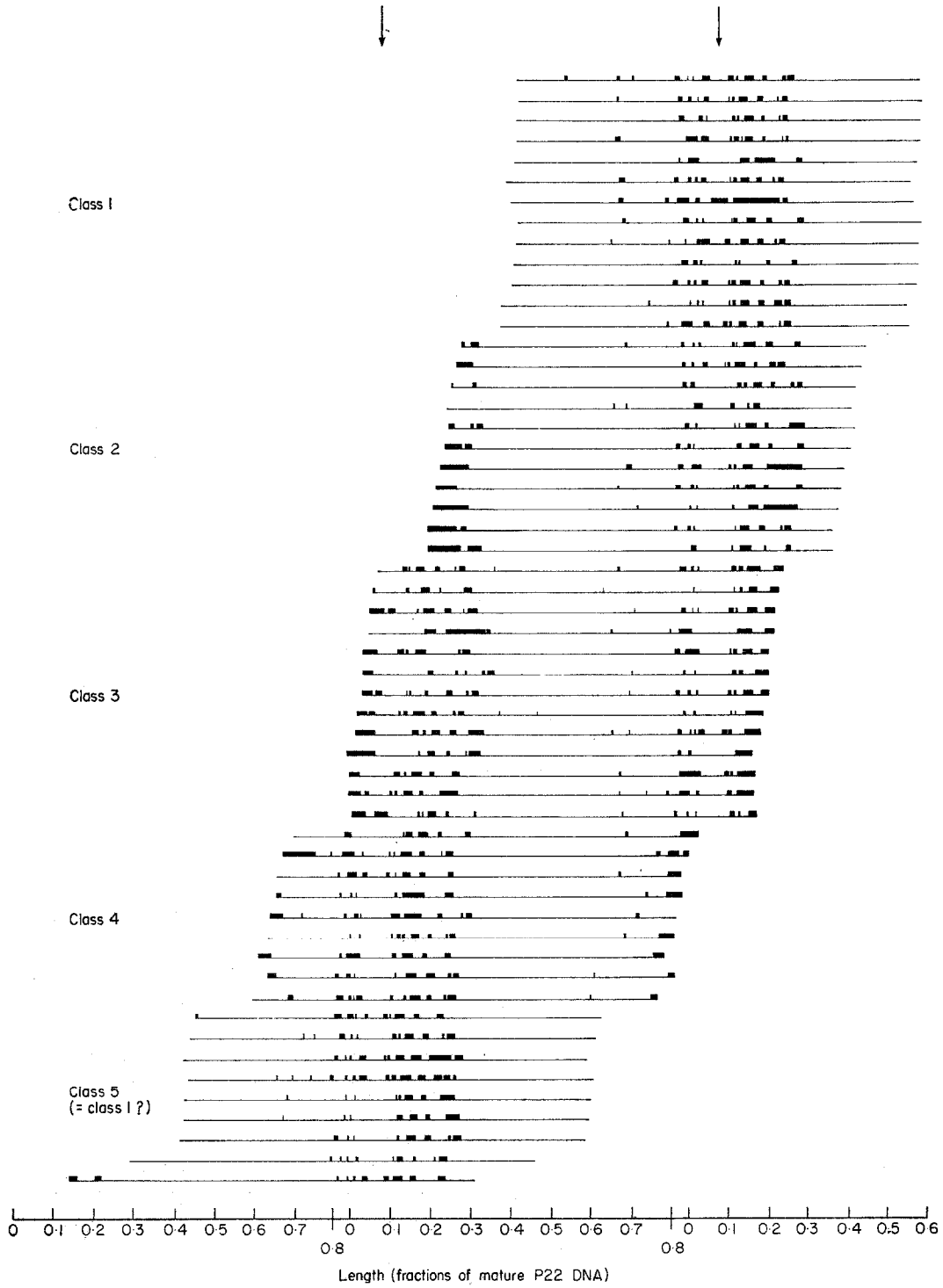
Class 1
Class 2
Class 3
Class 4
Class 5
(= class 1 ?)
0 0·1 0·2 0·3 0·4 0·5 0·6 0·7 0 0·1 0·2 0·3 0·4 0·5 0·6 0·7 0 0·1 0·2 0·3 0·4 0·5 0·6
0·8
0·8
Length (fractions of mature P22 DNA)

FIG. 9.

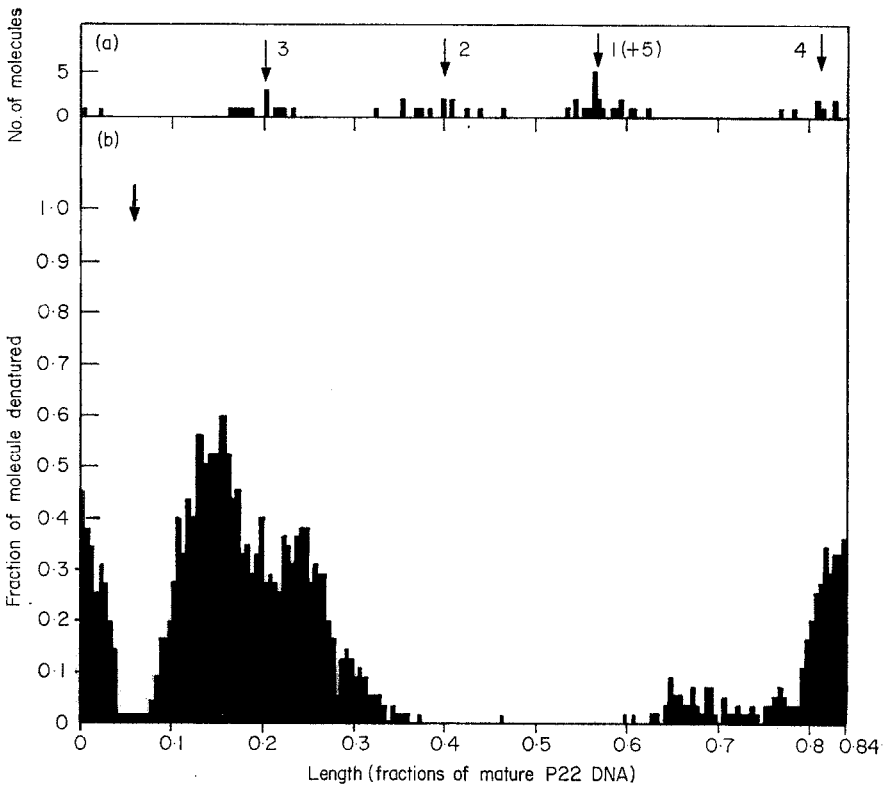

FIG. 10. (a) Histogram of the distribution of the ends of the molecules with respect to the denaturation map. The positions of ends are positions of the right ends of the molecules in Fig. 9. The ends are clustered into 4 classes, but there could be more (see Fig. 9).

(b) Histogram of the partial denaturation maps of P22*bp5* DNA (Fig. 9). The map range is plotted as 84%, since the TR value of P22*bp5* is estimated to be about 16%. This is done by taking out the TR of 16% from the left end of each molecule.

The fact that discrete classes are readily resolved in the P22*bp5* histogram makes it likely that there is only one starting point for cutting. If there were two or more starting points, discrete classes might not be expected and, if found, should in any case not be separated by a distance that approximates the terminal repetition. Of course, due to the limit of resolution, one cannot eliminate the possibility of clustered starting points within a relatively small region. Once again, as in the case of P22*bp1* DNA, ends are found to fall within both (G + C)-rich and (A + T)-rich regions.

FIG. 9. Partial denaturation maps of P22*bp5* DNA denatured at pH 11·32 for 30 min at room temperature. The length distribution of the 55 molecules measured is (100±8·5)%. The arrow indicates the reference for the alignment. Classes of molecules are grouped in such a way as to demonstrate that there could be more than 4 classes of molecules (as shown in the histogram in Fig. 10). The ends of molecules in class 5 differ only very slightly if at all from those in class 1.

(e) *Limited permutation in P22Tc-10 single strands*

The tetracycline-resistance transducing phage P22Tc-10 has an insertion of 20% of foreign DNA in the phage genome. This results in a terminal repetition of —18% (see Table 4 of the preceding paper). The position of the insertion is known to be located near *int* because of the loss of the *int* function in the deletion revertants of Tc-10 (Chan *et al.*, 1972). Since the tetracycline-resistance insertion has a characteristic self-complementary stem and loop structure, we can make use of this characteristic feature of the single-stranded Tc-10 DNA as an independent reference for lining up the molecules. The distribution of ends can then be studied using an independent method of lining up the DNA molecules. The major disadvantage of this method of lining up is that there is no distinction between left and right; furthermore, if the ends happen to fall within the stem and loop region, those molecules may not be detected. Nevertheless, as shown in Figure 11, when 37 single-stranded Tc-10 DNA molecules are lined up with respect to the position of the stem and loop structure, three discrete classes of molecules can be discerned. More classes might be created if some of these molecules were inverted. The resolution of discrete classes in the Tc-10 DNA is consistent with the finding of the partial denaturation maps of P22*bp*5 DNA. In both cases, the molecules fall into classes each separated from the next by a distance that approximates the terminal repetition.

(f) *Denaturation and self-reannealing experiments*

An independent demonstration of the relation between circular permutation and terminal repetition was given by denaturation–self-reannealing experiments using DNAs with different amounts of terminal repetition. We showed in the preceding paper that on denaturation and self-reannealing, circularly permuted molecules will form homoduplex circles with two single-stranded branches. The circumference of the circle equals the phage genome length; each single strand protruding from the circumference corresponds to the length of the terminal repetition. The distance between the two single strands is a measure of the staggering in permutation between the two reannealed single strands.

In order to demonstrate the relation between circular permutation and terminal repetition, DNAs extracted from wild-type P22, P22*bp*1, and P22*bp*5 mature phage were used, each having a terminal repetition of approximately 2%, 7% and 16%, respectively. Under our experimental conditions, more than 50% of the DNA was renatured; about equal numbers of circular and linear species were found in the renatured preparations.

Histograms of the ratio of the longer distance around the circle between the two branch positions of a renatured circular molecule divided by the circumference of that circular molecule are plotted in Figure 12 (see Lee *et al.*, 1970); the higher the ratio, the shorter the distance is between the branches. Figure 12(a) shows the distribution of branch distances in a population of homoduplex DNA circles formed from the wild-type P22 phage DNA. There is a non-uniform distribution of phase differences in the population of wild-type P22 DNA molecules, 92% of the circular molecules have their branch positions within 20% of one another. In contrast, in Figure 12(b) there is an almost uniform distribution of branch distances in a population of P22*bp*1 DNA molecules. There is an empty region between 0·92 and 1·0, as if none of the paired molecules in the population has branch positions closer than 8% or farther than 92% from each other.

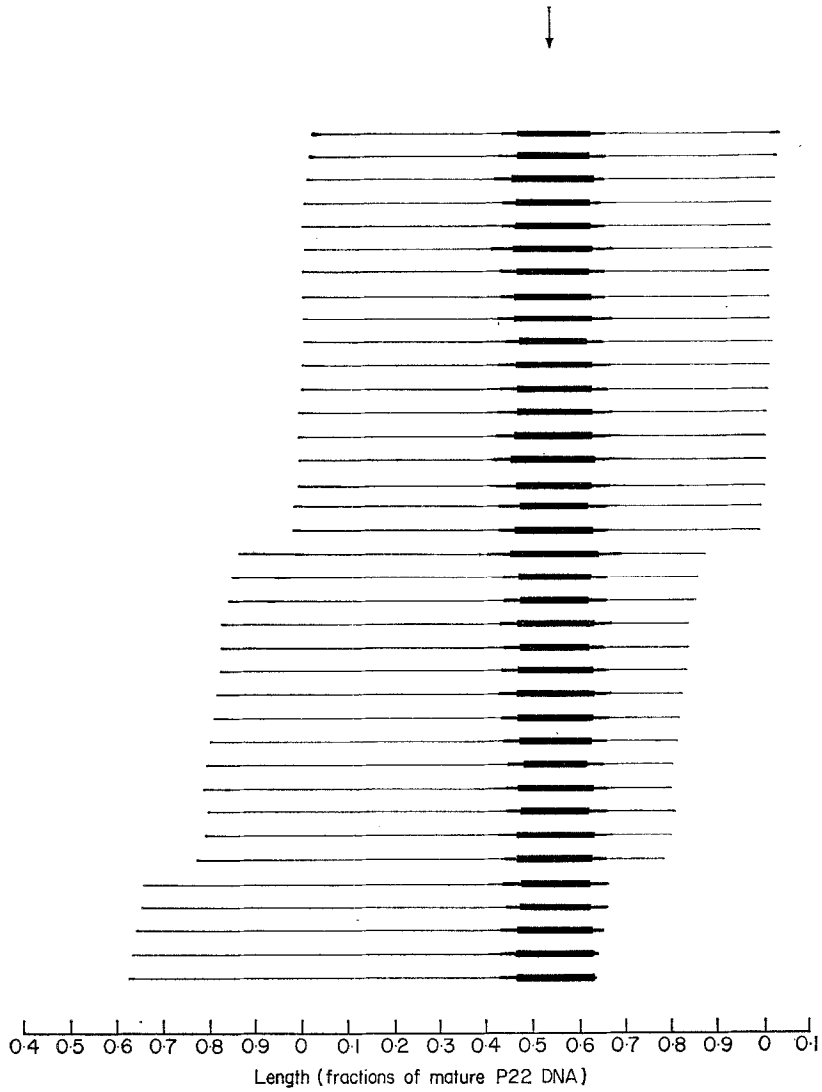

FIG. 11. Distribution of ends of the P22Tc-10 single-stranded DNA using the lariat-like structure of the tetracycline-resistance insertion† as the reference for the line-up. The length distribution of the 37 molecules measured is (100±7·2)%. Three classes are found but not all classes are represented, since molecules with ends that fall within the lariat structure were not detected and molecules can be flipped over to create more classes. The thick bars represent the loop region and the thin bars represent the stem region of the lariat-like structure. The conditions for intramolecular annealing are described in the preceding paper.

† Refer to Plate II(b) and Fig. 1(b) in the preceding paper (Tye *et al.*, 1974).

The uniform distribution of branch distances in the P22*bp5* homoduplex DNA circles (Fig. 12(c)) is similar to that found in P22*bp1* (Fig. 12(b)) except for the absence of the empty region between 0·92 and 1·0. This difference in the two profiles can be explained by what is known about branch migration and the number of possible sequential cuts (see Discussion).

The findings in the distribution of ends by the denaturation–self-reannealing

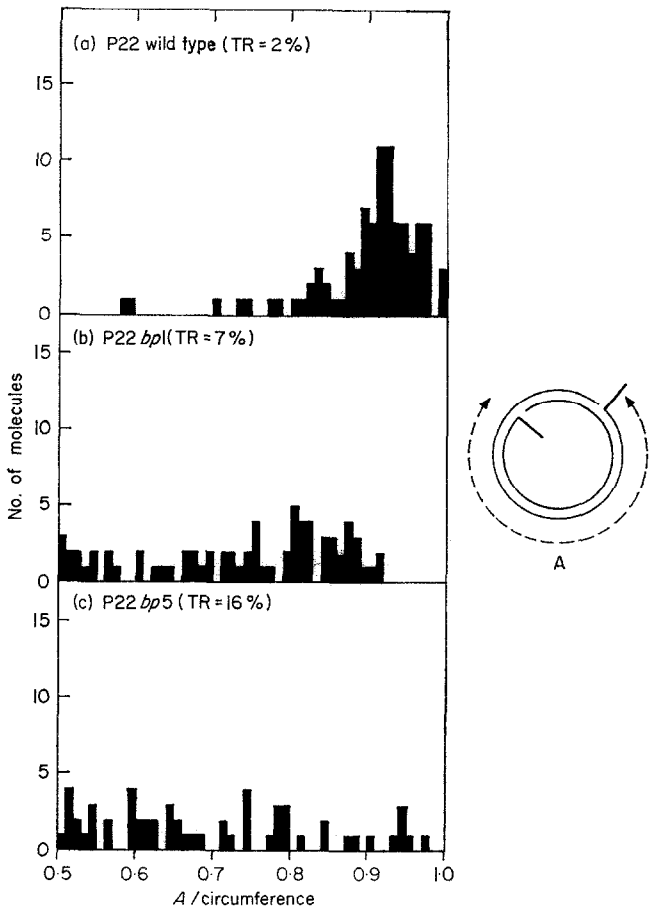

FIG. 12. Histograms of the quantity A/C, which is the longer distance between the 2 single-stranded branches of a renatured circular molecule divided by the circumference of that circular molecule.

(a) Histogram of A/C of the renatured circular molecules of P22 wild-type DNA (refer to Plate IV(a) in Tye *et al.*, 1974).

(b) Histogram of A/C of the renatured circular molecules of P22*bp*1 DNA (refer to Plate IV(b) in Tye *et al.*, 1974).

(c) Histogram of A/C of the renatured circular molecules of P22*bp*5 DNA (refer to plate IV(c) in Tye *et al.*, 1974).

technique confirm the findings by partial denaturation mapping. Both methods show that permutation in P22 wild-type DNA is limited to 20% of the map; an increase in the amount of terminal repetition increases the extent of permutation. Thus, both types of experiments clearly demonstrate the direct relation between terminal repetition and the extent of permutation predicted by the unique initiation–sequential encapsulation model.

4. Discussion

The evidence presented above shows that circular permutation in mature wild-type P22 DNA is not random. By two different methods, the ends of the DNA molecules in wild-type phage particles were found all to lie within a region extending over

about 20% of the genome. Furthermore, using the deletion and insertion mutants described in the preceding paper (Tye *et al.*, 1974), we have established that the extent of circular permutation in mature P22 DNA molecules depends directly and quantitatively on the size of terminal repetition. The preceding paper showed that the extent of terminal repetition is, in turn, determined directly and quantitatively by the genome size; i.e. by the total length of the non-repeated part of the genetic material of the phage in question.

In the course of presenting these results, a model that completely accounts for these results was presented (Figs 1 and 6). The model is the Streisinger headful encapsulation model (Streisinger *et al.*, 1967) with a few additional specifications.

(1) Each molecule of intracellular precursor DNA (concatemer), which is envisioned as an end-to-end polymer of the phage genome, is limited in size, and can provide a maximum of about ten headfuls.

(2) Encapsulation of headfuls of DNA begins at a unique site on each concatemer.

(3) After the first headful, subsequent headfuls are filled sequentially from the end left by the previous headful without any further specificity.

This model explains the results showing dependence of the extent of permutation on the size of the terminal repetition (see Fig. 6). Since encapsulation of the second headful starts where the first ended, the beginning of the second will be displaced from the beginning of the first by the length of the terminal repetition. If only ten headfuls are possible, then the tenth headful will be displaced by 18% from the first if the terminal repetition is 2% (as in wild-type P22 DNA), and by 63% if the terminal repetition is 7% (as in P22*bp*1 DNA).

(a) *The size of the intracellular precursor DNA*

From the partial denaturation map of wild-type DNA, the distribution of ends is about 20%, which would imply that a maximum of ten sequential headfuls is cut from the concatemer. For the *bp*1 partial denaturation map, the distribution of ends is about 60%, which would imply a maximum number of eight to nine sequential headfuls. In the histograms of the ratio of the longer distance between the branches divided by the circumference (A/C) in P22 wild-type circular molecules (Fig. 12(a)), the majority (92%) of the population fall within 20% of each other. This again suggests ten headfuls. In the histogram of A/C in *bp*1 (Fig. 11(b)) and *bp*5 (Fig. 11(c)), the calculation (see section on branch migration) for the phase difference in the population sets an upper limit of 12 headfuls in P22*bp*1 and a lower limit of six in P22*bp*5.

We conclude that the maximum number of sequential headfuls cut from a single concatemer is about ten. This result is in good agreement with previous investigations (Botstein, 1968; Botstein & Levine, 1968*a*; Botstein *et al.*, 1973) concerning the physical size of P22 DNA concatemers as measured by sedimentation analysis. In these studies, concatemer lengths ranging from two to ten times the mature length were found. Significantly, the maximum concatemer lengths were found not in wild type but in DNA maturation-defective mutants; these were about ten mature DNA lengths (Botstein & Levine, 1968*a*; Botstein *et al.*, 1973).

(b) *Direction of sequential encapsulation*

In the denaturation histograms of *bp*1 (Fig. 8), there seems to be, in the distribution of ends on the map, a decrease in the number of ends as one proceeds from right to

left. In the histogram of *bp5* (Fig. 10), the ends seem to cluster into four classes. The most abundant class (class 1) has 20 molecules, classes 2 and 3 have 13 molecules each, class 4 has nine molecules: again, there is a decrease of number in one direction; the same direction as observed in *bp1*, i.e. from right to left.

We conclude from this that there is competition between DNA replication and encapsulation or DNA degradation and encapsulation such that each sequential headful is more probable than the following one. Then the direction in which the number decreases in the distribution is the direction of the sequential cutting. The most frequent headful, in this view, represents the first one cut from the concatemer. This is consistent, of course, with the finding that the right side (but not the left) of these distributions (see especially *bp1*) coincides with the point on the map at which the wild-type ends cluster (Fig. 13).

(c) *Location of the* bp5 *and* bp1 *deletion substitutions*

Since the DNA from the deletion and wild-type DNA should have very similar denaturation maps differing only in the region of substitution and deletion, a comparison of these maps (Fig. 13) may indicate where the deletion is with respect to the denaturation map. All of the denaturation histograms shown have three major peaks. When all these histograms are lined up with one another with respect to the two major peaks, the third major peak appears to be successively displaced in the two deletion phage.

P22*bp1* has a net deletion of 5% with respect to the wild-type P22 and a substitution of 10% (Tye *et al.*, 1974). When lined up with respect to the first two major peaks, the third peak in the *bp1* histogram (Fig. 13(b)) is shifted about 5% towards the major peaks 1 and 2. Also, the shape of peak 2 is somewhat different from that of the wild-type peak (Fig. 13(b)). It seems as though the deletion–substitution occurs anywhere between peak 2 and peak 3.

P22*bp5* DNA has a 9% deletion with respect to P22*bp1* DNA, and 14% with respect to P22 wild type. The third peak in the *bp5* denaturation histogram (Fig. 15(c)) appears to be shifted even more (about 9%) towards the two major peaks. Again, it seems clear that the deletion occurs between peaks 2 and 3.

(d) *Location of the unique encapsulation–initiation site*

In all the phages examined, the initial headful appears to occur at the same place (in a (G + C)-rich region) with respect to the denaturation maps (Fig. 13). This result by itself strengthens the case for the sequential encapsulation idea and the unique direction of encapsulation. One can inquire into the genetic location of this site. Since we know that the *bp1* and *bp5* deletions remove the *int* and *att* loci (Chan *et al.*, 1972), we can use the deletion point as a reference between the denaturation and genetic maps. However, we can not tell by this means, left from right; another reference point is required. The one reference point, however, leaves two possibilities for the region in which the encapsulation–initiation point might be on the genetic map. From Figure 13, it is clear that the site is some 65% of the map away from the *int att* deletions. This places the site either near genes *13*, *19* and *3* (lysis and the first of the head genes; Botstein *et al.*, 1972) or near the major head encapsulation genes (genes *5*, *8* and *10*).

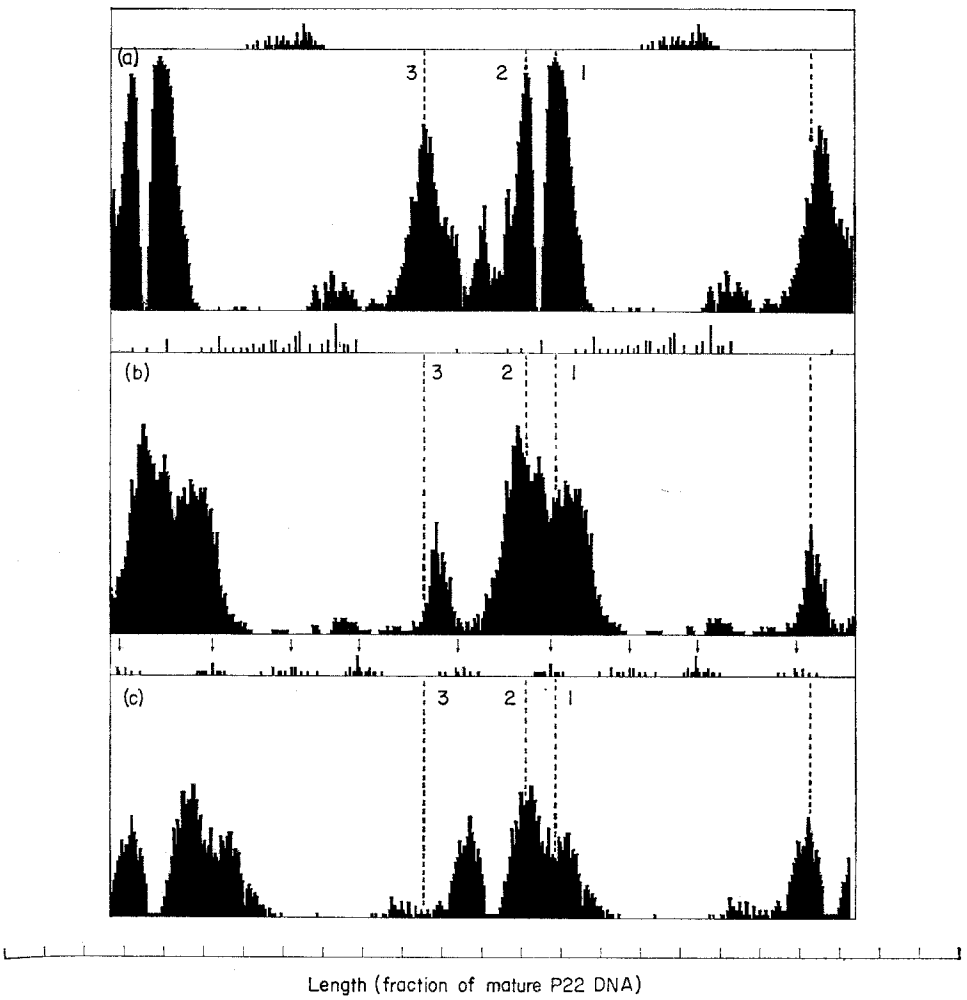

FIG. 13. Histograms of the partial denaturation maps of (a) P22 wild-type DNA (2% TR), (b) P22*bp*1 DNA (7% TR), (c) P22*bp*5 DNA (16% TR). The histograms are plotted as double map lengths for an easier comparison of the profiles of these histograms. The histograms are lined up with one another by the 2 major denaturation sites marked 1 and 2. A comparison of these histograms shows:

(i) the relation between the extent of permutation and the size of the TR;

(ii) that the most frequent headfuls are the first headfuls; this is strengthened by the fact that they all coincide at the same region of the partial denaturation map;

(iii) the *int*$^-$ deletion occurs between peaks 2 and 3;

(iv) there is a unique initiation site for DNA encapsulation in the (G + C)-rich region of the map, and this is approximately 65% away from the *int* deletion site;

(v) encapsulation seems to proceed sequentially and unidirectionally from right to left, since the number of headfuls decreases unidirectionally from right to left both in *bp*1 and in *bp*5.

(e) *Detection of discrete permutation classes in P22*bp*5 DNA*

As expected from our model, we found discrete classes in the case of phage with terminal repetitions that displace adjacent headfuls a distance large enough for us to detect. P22Tc-10 (−18% terminal repetition) gave discrete classes about 18% apart. P22*bp*1 (7% terminal repetition) gave a hint of classes 7% apart; these are only marginally detectable. However, P22*bp*5 (16% terminal repetition) gave four classes 17 to 24% apart. Unfortunately, given an 84% total genome, one would expect five classes 16% apart.

This discrepancy, though minor, requires explanation; three possibilities are offered.

(1) Our measurement of the terminal repetition (and of the genome size) has a standard error: in the preceding paper, we estimated the repetition as $16{\cdot}4 \pm 2$. Thus, our standard error is just large enough to be consistent with a real terminal repetition of 18 to 20%, which would give an expected four classes. Furthermore, as discussed in Materials and Methods, our estimates of terminal repetition depend on the measurement of single-stranded DNA, which we believe is more likely to be underestimated rather than overestimated.

(2) There might be a real variation in the headful length amounting to some 2 to 3% of the total P22 DNA length. If this were so, then sequential headfuls would propagate this variation, making the median position of each P22*bp*1 headful class successively more difficult to estimate.

(3) There might be a small amount of DNA hydrolyzed or skipped between successive headfuls. If this amount were small (less than about 2% of P22 DNA), this might account for our result.

(f) *Branch migration*

Branch migration was first described by Lee *et al.* (1970) in their analysis of coliphage 15 terminal repetition. As shown in the preceding paper, our denatured and reannealed DNA homoduplexes show branch migration. This phenomenon affects our results as follows.

(i) *Loss of discrete headful classes*

The distance between the two single-stranded branches can vary up to twice the length of the terminal repetition, since each branch can strand migrate as shown in Figure 14(a). Thus, no discrete classes are expected.

However, this increased variation in interbranch distance does not affect the conclusion that permutation is less limited in P22*bp*1 (7% terminal repetition) than in P22 wild type. If, in a population of P22*bp*1 DNA molecules, the distribution of ends were actually the same as in wild type P22 DNA, i.e. a 20% distribution, then a 7% terminal repetition in P22*bp*1 would allow branch migration that can increase variation over a range of 14% (Fig. 14(a)). One would then expect the distribution of interbranch distances to cover 34% of the map; but a uniform distribution of interbranch distances is actually found.

(ii) *Absence of interbranch distances less than one terminal repetition in length in P22*bp*1 homoduplex circles*

Strands annealed from successive headfuls (displacement = 1TR†) cannot circularize. Even if such a molecule managed (by fraying of the ends) to circularize,

† Abbreviation used: TR, terminal repetition.

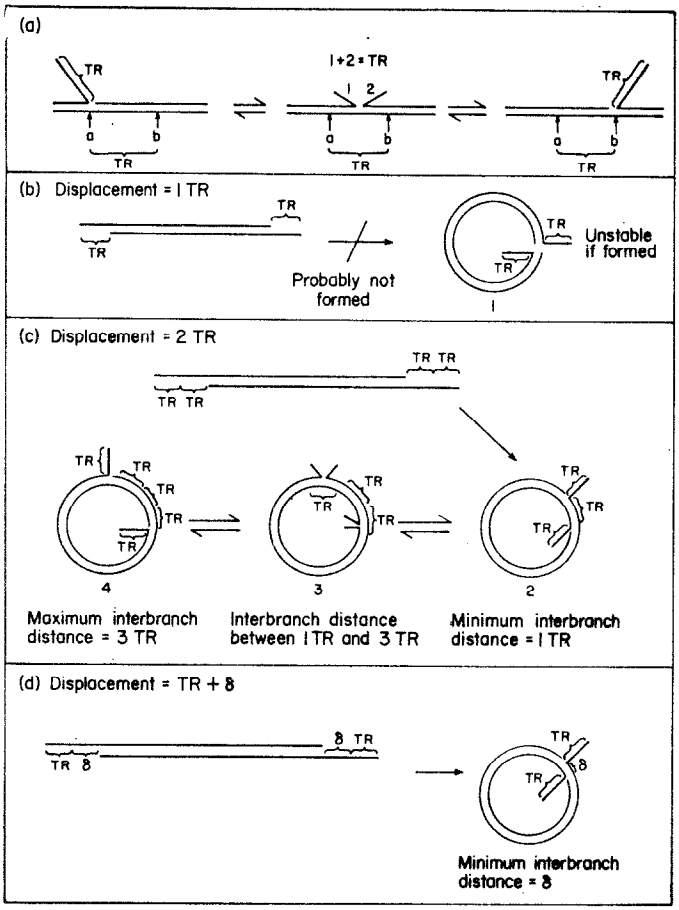

FIG. 14. Diagrams illustrating:
(a) the mechanism of branch migration;
(b) circularization cannot take place between 2 annealed strands that are displaced from each other by less than or equal to 1TR;
(c) circularization between 2 annealed strands that are displaced from each other by 2TR and the branch migration that can take place after circularization;
(d) circularization between 2 annealed strands can take place as long as the displacement of the 2 strands is greater than 1TR.

the circular form would be unstable, because of strand migration back to the configuration of no homology shown in Figure 14(b).

Since adjacent headfuls cannot donate strands to a reannealed circle, the smallest displacement yielding circles on denaturation and reannealing is 2TR. By strand migration, the minimum interbranch distance is, in this case, 1TR, and the maximum is 3TR (Fig. 14(c)).

These considerations account for the absence in the P22*bp*1 self-reannealing experiment (Fig. 12(b)) of interbranch distances less than 8%, since the TR value of P22*bp*1 is 7%.

An exception to this expectation concerns terminal repetitions large enough so that ten sequential headfuls reaches beyond 100% permutation. If the TR value is, for example, 16% (as in P22*bp*5), then the seventh headful is 96% displaced from the

first (see Fig. 6). However, the genome of P22*bp*5 is only 84% of the P22 wild-type genome in length. Thus, the net displacement of the seventh headful from the first in P22*bp*1 is 12% (not a multiple of 16). The third headful of P22*bp*1 is 32% displaced from the first; its net displacement with respect to the seventh headful is thus 20%. Annealing of strands from these two headfuls will produce circular forms; as shown in Figure 14(d), the minimum interbranch distance will be 4%.

From these considerations, we can show that the maximum number of headfuls from a concatemer in P22*bp*1 is 12, and that the minimum number in P22*bp*5 is six, since interbranch distances less than 1TR are *not* found in P22*bp*1 but they *are* found in P22*bp*5.

(g) *The excluded volume effect*

Clustered distribution of branch separation in denaturation–self-reannealing experiments has been observed in P1 DNA (Ikeda & Tomizawa, 1968) and coliphage 15 DNA (Lee *et al.*, 1970). In the denaturation–self-reannealing experiment, Lee *et al.* argued that the coliphage 15 chromosomes should be continuously permuted, and explained their observation of clustered ends by what is known as the "excluded volume" effect, i.e. it was proposed that in the renaturation of a population of circularly permuted molecules, strands with beginning points near each other preferentially nucleate and thus preferentially renature with each other. We have shown that for P22*bp*1 DNA, which has a deletion of 5% and a terminal repetition of 7%, the distribution of branch separation is no longer clustered in the renatured circular homoduplex. Even with the allowance for a maximum range of 14% for branch migration, one would not expect to find a uniform distribution of branch separations if the excluded volume effect were an important factor in this technique. On the contrary, without becoming involved in the theory, we find that the distribution of branch separation in the renaturation of a population of circularly permuted DNAs is, under our conditions, a direct measure of the extent of permutation in the population.

(h) *Nature of the unique initiation site for DNA encapsulation*

The interesting question with regard to the initiation of encapsulation is whether the unique initiation site for encapsulation is a unique base sequence or a physically unique structure such as a free end. If the unique site were a unique base sequence, there would be sequence specificity, which signals the encapsulation mechanism to start packaging. On this hypothesis, the first encapsulation event from a concatemer would be different from the subsequent events in the sense that the subsequent events show no sequence specificity. However, if the unique site were physically unique to begin with (for example, a free double-stranded end), then every encapsulation event would be identical; in all cases, the same substrate would be acted upon by the mechanism.

A simple model presents itself from the assumption that the multiple-length intracellular precursor is the product of an asymmetric replication mechanism such as the rolling circle (Gilbert & Dressler, 1968). One can then easily imagine that the end of the tail of the rolling circle (which is a specific sequence) may also be the unique free end at which DNA maturation begins. The fact that encapsulation

appears to proceed unidirectionally may thus reflect simply the structure of such an asymmetric replicative intermediate.

(i) *Generalized transduction*

The mechanism by which DNA is packaged is thought to be related to the transducing activities of the phage. Many phage capable of generalized transduction contain permuted phage DNA molecules. In these cases, one can consider the production of generalized transducing particles as a natural consequence of the packaging mechanism. Phage with unique DNA such as λ, which packages by sequence specificity (Wang & Kaiser, 1973), would be unlikely to package host DNA (although now it appears that λ has a very low generalized transducing activity: R. Weisberg, personal communication).

In generalized transducing phage like P22, if headful packaging is completely random, then one would expect as many transducing particles as infectious particles in any single burst, since there is at least as much host DNA as phage DNA in an infected cell. The fact that the frequency of generalized transducing particles is only about 5% (Ebel-Tsipis *et al.*, 1972) can be explained by a specificity for free ends, and the frequency of transduction would then reflect the number of free duplex ends in the host DNA and not the amount of host DNA.

In a single-burst analysis of the production of P1 infectious and transducing particles, Harriman (1972) found that only a fraction of the infected cells produces transducing particles as well as infectious particles. By using prophages λ, 21 and 186 as genetic markers, he found that the frequency of coproduction of markers on the same chromosome may be related to the distance between the markers. Harriman suggested that his data might be explained by the sequential headful packaging mechanism with the encapsulation–initiation site being any free duplex end. Cells that are capable of producing transducing particles are those in which the host chromosome has been broken to provide the encapsulation–initiation site. The majority of the cells have intact circular chromosomes, thus lacking sites for encapsulation of host DNA, and so cannot produce transducing particles. The higher frequency of coproduction for markers closer together on the host chromosomes is then expected.

The sequential model can also explain the observation made by Ozeki (1959) on the transduction of *Salmonella typhimurium* by phage P22. He observed that certain linked markers appear to be unlinked in transduction. If a preferred breakage point on the chromosome were near these markers, our model would anticipate preferential unlinkage of this kind.

Zinder (1955) showed that phage populations obtained at various times after infection of donor cells have different capacities to transduce given markers. This variability presumably reflects differences in the availability of fragments carrying these markers at different times during the course of phage growth, and may indicate that disruption of the donor chromosome occurs in some non-random manner.

Schmieger (1972) isolated mutants of phage P22 that show increased frequency for generalized transduction. He proposed that the product of this high transduction gene is a nuclease that cuts the host DNA. If mutation in the high transduction gene alters the activity of this enzyme such that it acts at many points, then an increase in the number of free ends would increase the frequency of transduction if sequential cutting can start from any free end.

(j) *Implications for the mechanism of DNA encapsulation*

The cutting of DNA concatemers into P22 headfuls has been shown to require the prior assembly of a head precursor called the prohead (Botstein *et al.*, 1973; King *et al.*, 1973). This prohead contains only six proteins, two of which are not essential to encapsulation and the cutting of concatemers. During the encapsulation process, one of the two major protein components of the prohead (the product of gene *8*) is removed. Further, the encapsulation process requires, in addition to a functional prohead, the action of two other P22 late gene products (those of genes *2* and *3*), neither of which appears to form part of a head-related structure. There is some evidence suggesting that the product of gene *3* might specify or control the nuclease responsible for the cutting of the concatemer (Botstein *et al.*, 1973; H. Schmieger, personal communication). Thus, the mechanism that accomplishes the sequential encapsulation of DNA from the concatemer is apparently quite simple and the sequence of events is relatively well understood.

(*k*) *Generality of the sequential packaging mechanism*

The sequential packaging mechanism is a far more efficient and economical way of packaging phage DNA than a random packaging mechanism. It is not known how general a packaging mechanism it is among permuted phage. Even in phage that have unique ends, a sequential packaging mechanism cannot be ruled out (Emmons, 1974). It is most likely that P1 and the coliphage 15 have packaging mechanisms similar to that of P22 (Ikeda & Tomizawa, 1968; Lee *et al.*, 1970) because of the clustering of interbranch distances in self-reannealed homoduplexes. Even with the T-even coliphages, the possibility should be considered that DNA is encapsulated in a manner similar to P22. MacHattie *et al.* (1967) showed how circular molecules formed by the annealing of denatured T2 DNA indicate that the number of different permutations is large and that there is no preferred permutation in the population. This kind of observation would be expected if sequential cutting can begin at any point on the concatemeric DNA or if sequential cutting does indeed start from a unique point but the expected limitation in permutation is obscured by the occasional encapsulation of irregularly sized particles (2/3, 9/10, etc.), which package smaller headfuls of DNA (Mosig, 1968).

It may be worth noting that the sequential encapsulation mechanism may apply to an animal virus. Recently, Gerry *et al.* (1973) reported terminal repetition and limited circular permutation in the single-stranded DNA chromosomes of adeno-associated virus. Although, obviously, modifications of the P22 mechanism are needed to account for the very limited permutation and the single-strandedness of the DNA, the sequential encapsulation idea might be relevant.

We are indebted to D. Dressler and J. Wolfson who first suggested that P22 DNA denaturation maps might not show random permutation. We thank F. Stahl and G. Mosig for valuable discussions relating to permutation in T4 DNA, and R. K. Chan, M. Susskind, S. H. Tye and G. Weinstock for their general enthusiasm for this problem. We are grateful to E. R. Jensen, M. Eden and I. T. Young for their patient assistance with the computer. The computer facilities were supported by a grant from the National Institutes of Health (5P01GM14940-07) given to M. Eden and I. T. Young. This research is supported by grants from NIH (GM 18973-02) and the American Cancer Society (VC18B). One of us (D. B.) holds a Career Development Award from NIH (5K04GM7032502). Another author (B.-K. T) is supported by NIH grant no. CA12174-03. We thank Wanda Fischer for her assistance in preparing the manuscript.

REFERENCES

Baldwin, R. L., Barrand, P., Fritsch, A., Goldthwait, D. & Jacob, F. (1966). *J. Mol. Biol.* **17**, 343–357.

Botstein, D. (1968). *J. Mol. Biol.* **34**, 621–641.

Botstein, D. & Levine, M. (1968*a*). *J. Mol. Biol.* **34**, 643–654.

Botstein, D. & Levine, M. (1968*b*). *Cold Spring Harbor Symp. Quant. Biol.* **33**, 659–667.

Botstein, D., Chan, R. K. & Waddell, C. (1972). *Virology*, **49**, 268–282.

Botstein, D., Waddell, C. & King, J. (1973). *J. Mol. Biol.* **80**, 669–695.

Chan, R. K., Botstein, D., Watanabe, T. & Okada, Y. (1972). *Virology*, **50**, 883–898.

Ebel-Tsipis, J., Botstein, D. & Fox, M. S. (1972). *J. Mol. Biol.* **71**, 433–448.

Emmons, S. W. (1974). *J. Mol. Biol.* **83**, 511—525.

Frankel, F. (1966*a*). *J. Mol. Biol.* **18**, 109–126.

Frankel, F. (1966*b*). *J. Mol. Biol.* **18**, 127–143.

Frankel, F. (1966*c*). *J. Mol. Biol.* **18**, 144–155.

Freifelder, D., Kleinschmidt, A. K. & Sinsheimer, R. L. (1964). *Science*, **146**, 254–255.

Gerry, H. W., Kelly, T. J., Jr & Berns, K. I. (1973). *J. Mol. Biol.* **79**, 207–225.

Gilbert, W. & Dressler, D. (1968). *Cold Spring Harbor Symp. Quant. Biol.* **33**, 474–484.

Gough, M. & Levine, M. (1968). *Genetics*, **58**, 161–169.

Harriman, P. (1972). *Virology*, **48**, 595–600.

Hershey, A., Burgi, E. & Ingraham, L. (1963). *Proc. Nat. Acad. Sci., U.S.A.* **49**, 748–755.

Ikeda, H. & Tomizawa, J. (1968). *Cold Spring Harbor Symp. Quant. Biol.* **33**, 791–798.

Inman, R. B. (1967). *J. Mol. Biol.* **28**, 103–116.

Inman, R. B. & Schnös, M. (1970). *J. Mol. Biol.* **49**, 93–98.

King, J., Lenk, E. V. & Botstein, D. (1973). *J. Mol. Biol.* **80**, 697–731.

Kleinschmidt, A. K. (1968). *Methods in Enzymology*, **12**, 361–377.

Laemmli, U. K. (1970). *Nature (London)*, **227**, 680–685.

Lee, C. S., Davis, R. W. & Davidson, N. (1970). *J. Mol. Biol.* **48**, 1–22.

Luftig, R. B., Wood, W. B. & Okinaka, R. (1971). *J. Mol. Biol.* **57**, 555–573.

MacHattie, L. A., Ritchie, D. A., Thomas, C. A., Jr & Richardson, C. C. (1967). *J. Mol. Biol.* **23**, 355–363.

MacHattie, L. A., Rhoades, M. & Thomas, C. A., Jr (1972). *J. Mol. Biol.* **72**, 645–656.

Mandel, M. (1967). *Mol. Gen. Genet.* **99**, 88–96.

Mosig, G. (1968). *Genetics*, **59**, 137–151.

Ozeki, H. (1959). *Genetics*, **44**, 457–470.

Rhoades, M. & Rhoades, E. A. (1972). *J. Mol. Biol.* **69**, 187–200.

Rhoades, M., MacHattie, L. A. & Thomas, C. A., Jr (1968). *J. Mol. Biol.* **37**, 21–40.

Ritchie, D. A., Thomas, C. A., Jr, MacHattie, L. A. & Wensink, P. C. (1967). *J. Mol. Biol.* **23**, 365–376.

Salzman, L. A. & Weissbach, A. (1967). *J. Mol. Biol.* **28**, 53–70.

Schmieger, H. (1972). *Mol. Gen. Genet.* **119**, 75–88.

Showe, M. K. & Black, L. W. (1973). *Nature New Biol.* **242**, 70–75.

Skalka, A., Poonian, M. & Bartl, P. (1972). *J. Mol. Biol.* **64**, 541–550.

Smith, M. G. & Skalka, A. (1966). *J. Gen. Physiol.* **49**:6, part 2, 127–142.

Streisinger, G., Emrich, J. & Stahl, M. M. (1967). *Proc. Nat. Acad. Sci., U.S.A.* **57**, 292–295.

Thomas, C. A., Jr, Kelly, T. J., Jr & Rhoades, M. (1968). *Cold Spring Harbor Symp. Quant. Biol.* **33**, 417–424.

Tye, B. K., Chan, R. K. & Botstein, D. (1974). *J. Mol. Biol.* **85**, 485–500.

Wake, R. G., Kaiser, A. D. & Inman, R. B. (1972). *J. Mol. Biol.* **64**, 519–540.

Wang, J. C. & Kaiser, A. D. (1973). *Nature New Biol.* **241**, 16–17.

Wolfson, J., Dressler, D. & Magazin, M. (1972). *Proc. Nat. Acad. Sci., U.S.A.* **69**, 499–504.

Wu, R. & Kaiser, A. D. (1968). *J. Mol. Biol.* **35**, 523–537.

Wu, R. & Taylor, E. (1971). *J. Mol. Biol.* **57**, 491–511.

Yamagashi, H., Nakamura, K. & Ozeki, H. (1965). *Biochem. Biophys. Res. Commun.* **20**, 727–732.

Zinder, N. D. (1955). *J. Cell. Comp. Physiol.* (suppl. 2), **45**, 23–49.